



Secreted Gal-3BP is a novel promising target for non-internalizing Antibody–Drug Conjugates



Francesco Giansanti^{a,1}, Emily Capone^{b,1}, Sara Ponziani^{a,c}, Enza Piccolo^c, Roberta Gentile^c, Alessia Lamolinara^d, Antonella Di Campli^b, Michele Salles^b, Valentina Iacobelli^e, Annamaria Cimini^a, Vincenzo De Laurenzi^b, Rossano Lattanzio^b, Mauro Piantelli^c, Rodolfo Ippoliti^a, Gianluca Sala^{b,c,*,2}, Stefano Iacobelli^{c,*,2}

^a Department MESVA, University of L'Aquila, 67100 Coppito, Italy

^b Department of Medical, Oral and Biotechnological Sciences, University of Chieti-Pescara, Chieti, Italy

^c MediaPharma s.r.l., Via della Colonna 50/A, 66100 Chieti, Italy

^d Department of Medicine and Aging Cesi-Met, Via Polacchi 11, 66100 Chieti, Italy

^e Department of Gynecology & Obstetrics, Sapienza University of Rome, 00100 Rome, Italy

ARTICLE INFO

Keywords:

Non-internalizing ADC
Galectin-3-binding protein
Melanoma
Maytansinoid derivatives

ABSTRACT

Galectin-3-binding protein (Gal-3BP) has been identified as a cancer and metastasis-associated, secreted protein that is expressed by the large majority of cancers. The present study describes a special type of non-internalizing antibody-drug-conjugates that specifically target Gal-3BP. Here, we show that the humanized 1959 antibody, which specifically recognizes secreted Gal-3BP, selectively localized around tumor but not normal cells. A site specific disulfide linkage with thiol-maytansinoids to unpaired cysteine residues of 1959, resulting in a drug-antibody ratio of 2, yielded an ADC product, which cured A375m melanoma bearing mice.

ADC products based on the non-internalizing 1959 antibody may be useful for the treatment of several human malignancies, as the cognate antigen is abundantly expressed and secreted by several cancers, while being present at low levels in most normal adult tissues.

1. Introduction

The use of cytotoxic agents is at the basis of the medical treatment of cancer. Although these agents preferentially accumulate at the tumor sites, a certain amount reaches healthy organs, causing cytotoxic side effects. One possible solution to avoid or limit the lack of selectivity of cytotoxic agents is to couple them to an antibody to form an Antibody-Drug Conjugate (ADC) recognizing specifically a target antigen expressed at the cell surface that is unique to or expressed at higher levels in cancer cell types than in normal tissues [1]. This makes the ADC approach cell type specific and target specific. Unfortunately, several technical difficulties have been encountered with the ADC approach. A first drawback is that the targets have been limited to proteins/receptors that internalize upon ADC binding. In some cases, even though the target for the ADC exists on the cell surface, internalization does not

occur [2]. Complicating this even further are the cases where the target is expressed and internalization occurs, but the internalization is within compartments where drug antibody dissociation does not occur, leaving the drug ineffective [3]. Another difficulty encountered with the ADC approach relates to how much active drug can be delivered inside the cell. Indeed, payload distribution within the tumor is critical to predict ADC-based therapy efficacy. Huge efforts in the field of ADC development are addressed to generate novel compounds with ideal delivery to the site of action to maximize efficacy [4].

Given all these constraints, it is not surprising that there are only a few ADCs for application in oncology: Gemtuzumab ozogamicin (Mylotarg[®]), brentuximab vedotin (Adcetris[®]), trastuzumab emtansine (Kadcyla[™]), and Inotuzumab ozogamicin (Besponsa[®]) have been available on the market. Therefore, there continues to be a need for improved ADC that circumvents these requirements and/or overcome

* Corresponding author at: Department of Medical, Oral and Biotechnological Sciences, University of Chieti-Pescara, CESI-MET, Via dei Polacchi 11, 66100 Chieti, Italy.

** Corresponding author.

E-mail addresses: g.sala@unich.it (G. Sala), iacobelli@unich.it (S. Iacobelli).

¹ These authors contribute equally to this work.

² These authors share senior authorship.

the difficulties and drawbacks of existing methods.

Recently, a type of ADC which do not need to be internalized by cancer cells has been investigated. These non-internalizing ADCs target antigens that are structural components of the environment surrounding tumor cells. For example, reports have shown that ADCs based on site specific disulfide linkage with thiol-drugs directed against the alternatively spliced extracellular A domain of fibronectin, a component of the tumor subendothelial extracellular matrix, can mediate a potent anticancer activity in the mouse [5,6]. It has been postulated that disulfide-based ADC products may release their payload upon tumor cell death, in a process that can be amplified by the diffusion of the cleaved cytotoxic drug into neighboring cells and by the subsequent release of reducing agents (e.g. cysteine, glutathione) [7–11].

Galectin-3-binding protein (Gal-3BP, Uniprot ID – Q08380), also known as 90 k or Mac-2-binding protein is a large oligomeric, highly glycosylated protein that in humans is encoded by LGALS3BP gene [12,13]. The protein was originally described by our group while aiming to identify proteins secreted *in vitro* by human cancer cell lines, such as CG-5 (breast cancer) [14,15], or independently as a ligand of the lactose-specific S-type lectin, galectin-3 (formerly Mac-2) [16,17].

Accumulating evidence has shown that this protein may be involved in cancer growth and progression. Notably, significantly elevated expression of Gal-3BP in the serum or tumor tissues has been found to be associated with a poor clinical outcome in patients with a variety of cancer types [18–22]. Although the mechanism underlying these negative influences of Gal-3BP on the prognosis of various cancers is not well understood, it may be related to the multidomain nature of the protein and its association with different ligands in different tumor tissues. These interactions may support the well-characterized role of the protein in mediating cell-cell and cell-extracellular matrix [23,24] adhesion processes and, more recently, tumor angiogenesis [25,26].

Attempts to neutralize Gal-3BP functions have been investigated by monoclonal antibodies specifically directed against the different domains of the protein [27]. One antibody recognizing a conformational epitope along the lectin binding domain of Gal-3BP, named SP-2 has been generated and found to possess promising therapeutic activity in several tumor xenografts [25].

In this article, we attempt to evaluate whether Gal-3BP is a suitable target for non-internalizing ADC based cancer therapy. A humanized version of the murine SP-2 antibody, 1959 was generated and successively engineered (hereafter named 1959-sss) through cysteine to serine substitution into the hinge region allowing a site-specific, linker-less thiol-drug coupling at the residual C-terminal cysteines of the light chain. Three 1959-sss-based ADC products were obtained using as payloads the maytansinoid thiol-derivatives DM1-SH, DM3-SH and DM4-SH. We show that 1959-sss conjugated with DM3 (1959-sss/DM3) or DM4 (1959-sss/DM4), but not with DM1 (1959-sss/DM1) mediated a potent antitumor activity, including several cures, in a model of melanoma xenograft. Additionally, we show that 1959-sss/DM3 was completely stable *in vivo*, when tested in immunocompromised mice.

2. Materials and methods

2.1. Cell lines

Melanoma (A375m), neuroblastoma (SKNAS), hepatocellular carcinoma (Hep-G2) cells and human fibroblasts (BJ) were purchased from American Type Culture Collection (Rockville, MD, USA). Neuroblastoma Kelly cell line was purchased from Sigma-Aldrich (St. Louis, MO, USA). All cell lines were cultured < 3 months after resuscitation. The cells were cultured using DMEM (A375m and SKNAS) or EMEM (Hep-G2 and BJ) or RPMI (Kelly) media according to manufacturer's instructions, supplemented with 10% heat-inactivated fetal bovine serum (FBS; Invitrogen), L-glutamine, 100 units/ml penicillin, and 100 µg/ml streptomycin (Sigma-Aldrich Corporation, St. Louis, MO, USA), and incubated at 37 °C in humidified air with 5% CO₂.

2.2. Generation of 1959-sss

The murine anti-Gal-3BP SP-2 antibody [25] was humanized by CDRs grafting into an IgG1 scaffold as previously described [28,29]. Antibody variants were screened for antigen binding affinity by ELISA and the lead candidate was selected and named 1959. For site-specific conjugation, 1959 was engineered so that the cysteine residues of the heavy chain in positions 220, 226, and 229, were mutated into serine residues, as previously described (US 2008/0305044 A1) [30]. The full amino acid sequences for 1959-sss are given in Supplementary Fig. 1.

2.3. ADC generation

1959-sss antibody was reduced using 60 M excess of TCEP (Tris(2-carboxyethyl) phosphine (Thermo Fisher Scientific), in phosphate-buffered saline (PBS, Sigma-Aldrich), pH = 7.4. The reaction was carried out overnight at RT. The TCEP-reduced antibody in 100 mM phosphate buffer pH 7.4 was then incubated with 100 M excess of DTNB (5,5'-Dithiobis(2-nitrobenzoic acid; Sigma-Aldrich). The reaction was carried out overnight at RT and stopped by passing the 1959-sss/DTNB mixture through a G25 Sephadex column equilibrated in PBS/5% sucrose/10% DMA (NN' dimethyl acetamide, Sigma-Aldrich). The DTNB-derivatized 1959-sss antibody was then reacted with 10 M excess of thiol-maytansinoids DM1-SH, DM3-SH, or DM4-SH in PBS/5% sucrose/10% DMA overnight at RT. The reaction was stopped by adding 500 M excess iodoacetamide (Sigma-Aldrich). To eliminate unreacted free maytansinoid, the reaction mixture was passed through a G25 Sephadex column equilibrated in PBS/5% sucrose/10% DMA in an isocratic flow with a flow rate of 1 ml/min.

The final concentration of the ADCs was estimated by UV-VIS spectrophotometry, using an extinction coefficient $\epsilon_{280} = 1.6 \text{ M}^{-1} \text{ cm}^{-1}$. The thiol-maytansinoids DM1-SH, DM3-SH and DM4-SH were provided by Eisai (Eisai Inc, MA, USA).

2.4. Characterization of ADC

All ADC products were analyzed by SDS-PAGE and size exclusion chromatography (Superdex200 10/300GL; GE Healthcare). Release of free thiol-maytansinoids after the reduction with 60 M excess TCEP, was revealed by HPLC analysis using a C18 (Vertex plus, Knauer) column eluting the drugs with a linear gradient 0–100% of 0.1% TFA to 0.1% TFA/80% Acetonitrile detecting at 254 nm. The amount of released thiol-maytansinoid was estimated by extrapolation from a calibration curve obtained in the same conditions. After analysis of 500 µl (0.3 mg/ml) of non-reduced and reduced ADCs, the Drug-Antibody Ratio (DAR) calculated was 2.

Naked 1959-sss antibody and the ADCs were analyzed by HIC chromatography on a MabPac-Hic-Butyl column (ThermoScientific) equilibrated in 1.5 M Ammonium sulfate, 50 mM sodium phosphate pH 7.0, 5% isopropanol. The elution was obtained with a linear gradient 0–100% of 50 mM sodium phosphate pH 7.0, 20% isopropanol, 1 ml/min.

Naked 1959-sss antibody and the ADCs were further characterized by mass spectrometry performed by Toscana Life Sciences (<http://www.toscanalifesciences.org/it/>). After desalting with a PD Spin TrapG25, 2 µl of each sample were mixed with 2 µl of a s-DHB saturated solution in 0.1% TFA in distilled water /acetonitrile (50:50). Mixtures were deposited on a stainless-steel target and allowed to dry. Mass spectra were acquired using an Ultraflex MALDI TOF/TOF (Bruker, GmBH) in linear positive mode. In some measurements 1959-sss and the ADCs were reduced with excess TCEP before the analysis.

2.5. Therapy studies

Homozygous Balb/c nu/nu athymic female mice (4–6-week old) were purchased from Charles River Laboratories, Milan, Italy and

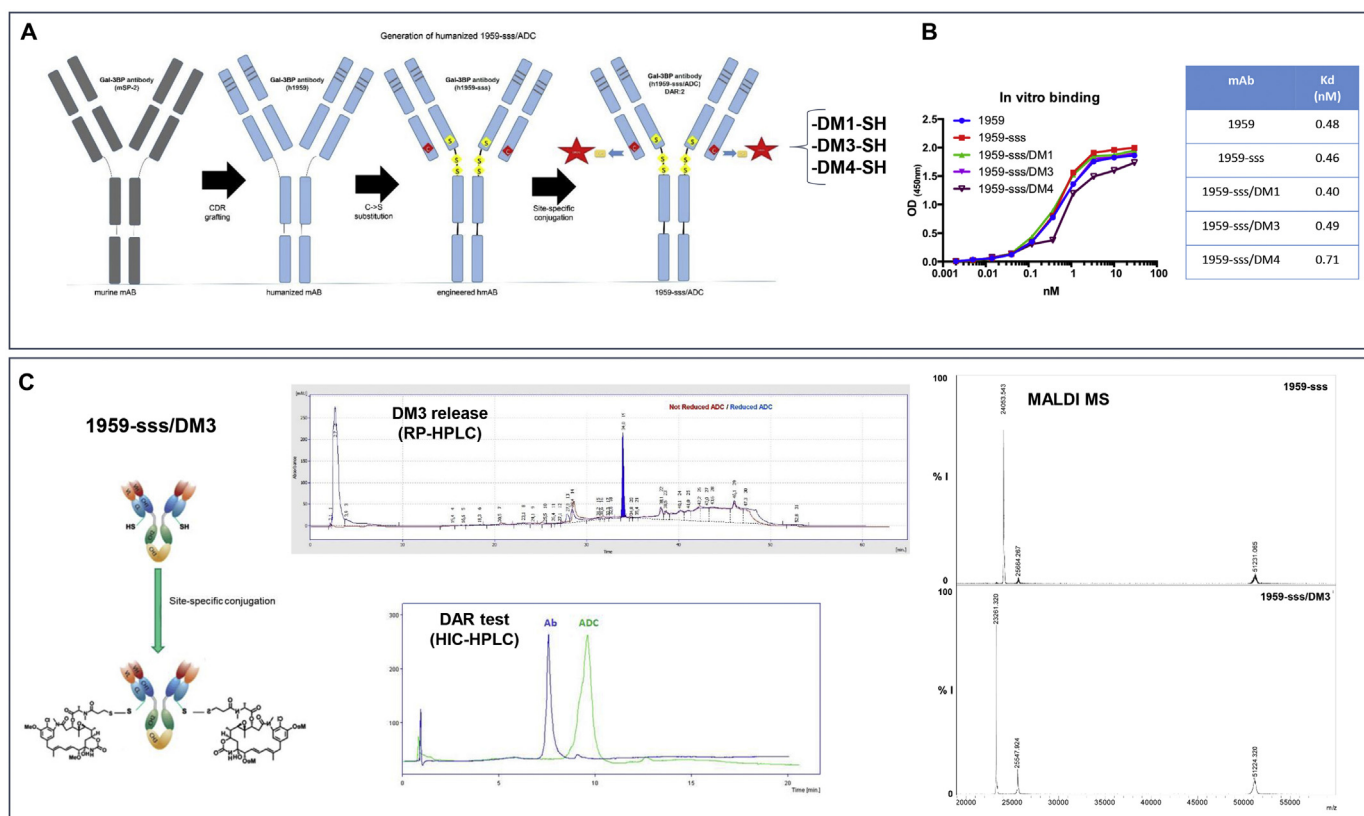


Fig. 1. Generation and characterization of 1959-sss/ADCs. (A) Schematic representation of 1959-sss based-ADCs generation; (B) in vitro binding affinity of 1959 wild-type, naked and conjugated 1959-sss antibodies. ELISA was performed using as capture antigen the recombinant purified GAL3-BP protein and bound 1959 antibodies were detected by HRP-labelled goat anti-human IgG. Kd values of mAbs were calculated using GraphPad Prism 5.0 software and are shown in the table. (C) Schematic representation and biochemical characterization of 1959-sss/DM3 by RP-HPLC, HIC-HPLC and MS. Free drug release was analyzed by inverse phase HPLC and confirmed by mass spectroscopic analysis showing a shift of 780 Da in the light chains corresponding to DM3 molecular weight. DAR test chromatograms revealed unconjugated 1959-sss (blue line) and 1959-sss/DM3 (green line). DAR = 2. (For interpretation of the references to colour in this figure legend, the reader is referred to the web version of this article.)

maintained at 22–24 °C under pathogen-limiting conditions as required. Cages, bedding, and food were autoclaved before use. Mice were given a standard diet and water ad libitum and acclimatized for 2 weeks before start of the experiments. Housing and all procedures involving the mice were performed according to the protocol approved by the Institutional Animal Care and Use Committee (Authorization n° 629/2015-PR).

Five million of exponentially growing A375m cells were implanted s.c. into the right flank of the mice. When tumors became palpable (approximately 150 mm³), animals were randomly divided and intravenously injected. Doses and schedules are described in the individual figure legends.

Tumor volume was monitored twice a week by a caliper and calculated using the following formula: tumor volume (mm³) = (length * width²)/2. A tumor volume of 1.5 cm³ was chosen as endpoint for all experiments after which mice were sacrificed and tumors dissected, fixed with formalin and embedded in paraffin.

2.6. Biodistribution studies

1959-sss/DM3 accumulation in tumor tissue was evaluated by immunofluorescence analysis of A375m tumor xenografts. Animals bearing A375m tumors (*n* = 3) received a single injection of PBS (as a control), or 1959-sss/DM3 at the dose of 10 mg/kg and thereafter animals were sacrificed 72 h later. Fresh tissues from heart, lung, kidney and tumor were frozen in a cryo-embedding medium (OCT, BioOptica) and cryostat sections were incubated with the following antibodies: rat monoclonal anti-CD31 (550,274, BD Pharmingen) mixed with rat

monoclonal anti-CD105 (550,546, BD Pharmingen) at 1:40 dilution, followed by secondary antibody (1:200 dilution) AlexaFluor-546 conjugated (A11081, Molecular Probes, Life Technologies) and AlexaFluor-488 conjugated (1:200 dilution) anti-human IgG (A11013, Invitrogen, Life Technologies). A mixture of antibodies against CD31 and CD105 was used to increase the probability of staining all of the tumor endothelium as previously reported [31]. Nuclei were stained with DRAQ5 1:1000 (62254, Alexis, Life Technologies). Images acquisition was performed using Zeiss LSM 510 META confocal microscope.

2.7. LC-MS (Liquid Chromatography Mass Spectrometry) analysis of released payload in mice serum

For the evaluation of free thiol-maytansinoid in mice serum, CD1 nude mice were injected intravenously with 10 mg/kg of 1959-sss/DM3 or equimolar amount of free DM3-SH. Blood samples were collected thereafter at the following time points (3 animals per time-point): 1 min, 5 min, 1 h, 24 h and 72 h. LC-MS analysis of the DM3-SH was performed by LC-MS by Toscana Life Sciences (<http://www.toscanalifesciences.org/it/>). Serum samples (100 µl) were treated with 200 µl of ACN:MeOH (50/50, v/v) in order to precipitate proteinaceous materials. The supernatant was recovered by centrifugation at 4000 x g for 20 min at 4 °C, evaporated to dryness under nitrogen stream. 100 µl of 0.1% formic acid in H₂O:ACN (90:10, v/v) was added to each vial. Samples (10 µl) were analyzed by HPLC-MS/MS using a CSH C₁₈ 130 Å column (1 mm × 150 mm, 1.7 µm, Waters), at 50 °C and with a flow rate of 0.1 µl/min in gradient mode. Mobile phase A consisted of 0.1% formic acid in water and mobile phase B of 0.1% formic acid in ACN.

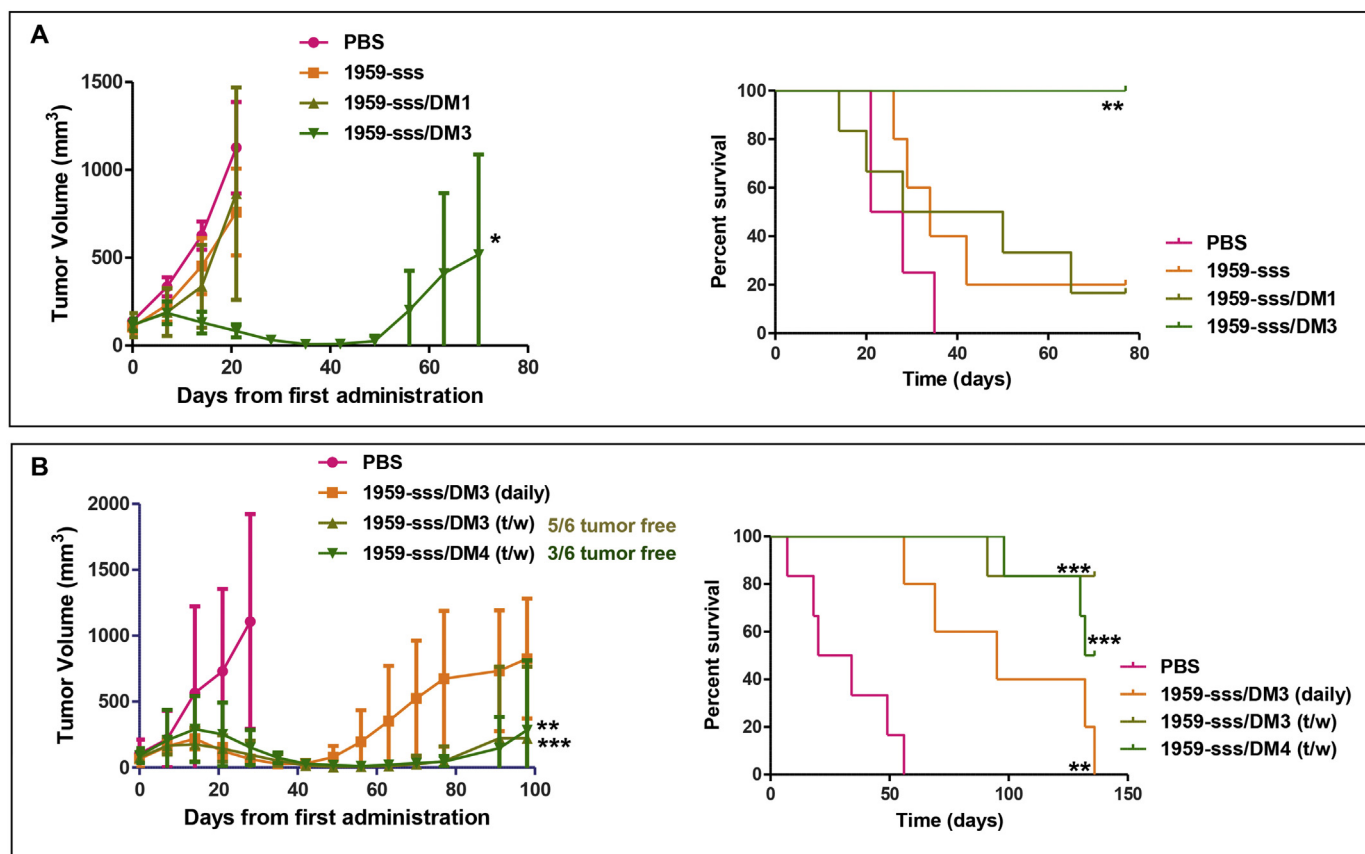


Fig. 2. 1959-sss-based ADCs show therapeutic activity against melanoma A375m xenograft. Tumor growth and Kaplan-Meier survival curves. (A) Melanoma A375m xenografts were established by subcutaneous injection of 5×10^6 cells in immunodeficient CD1 mice. When tumors reached a volume of ~ 150 mm³, mice were randomly grouped and intravenously injected with 10 mg/kg of naked 1959-sss, 1959-sss/DM1 or 1959-sss/DM3 daily for a total of 5 injections. $n = 5$ –6 mice/group; * $p = .0182$; ** $p = .0011$. (B) Established A375m melanoma xenografts were treated by intravenously injection with 10 mg/kg of 1959-sss/DM3 daily or twice weekly (t/w) for a total of five administrations, or with 10 mg/kg 1959-sss/DM4 twice weekly (t/w). $n = 6$ mice/group; ** $p = .0015$; *** $p = .0006$. Control groups received PBS. Survival curves evaluated by Kaplan-Meier and analyzed by the log-rank test using Graphpad Prism 5 software.

The following gradient was used: 10% B for 1 min, 10%–100% in 7 min, holding at 100% B for 1 min and re-equilibration at 10% B for 10 min. For each sample the LC-ESI-MS/MS runs were performed in triplicate. The detector was a Q-Exactive Plus mass spectrometer (Thermo Scientific) operating in positive ion mode with the following parameters: capillary temperature, 320 °C; spray voltage, 2.7 kV; sheath gas (nitrogen), 5, resolution, 70,000; AGC target, 2e5; Maximum IT, 100 ms; Isolation window, m/z 2.0; Scan range, m/z 150–2000; NCE, 24. Parallel reaction monitoring (PRM)-based targeted mass spectrometry was used to quantitative determination of DM3-SH. The protonated molecular ions at m/z 732.4909 was selected and the fragmentation pathway yielding the ion at 700.4639 was monitored. The acquisition software was XCalibur, version 3.0.63 (Thermo Scientific). The detection limit of free DM3-SH in the assay resulted to be 10 ng/ml.

2.8. Toxicity studies in rabbits

The acute toxicity of the 1959-sss/DM3 was investigated following intravenous injection of a single dose of 5 mg/kg of the ADC to one male and one female rabbit. The following investigations were performed: clinical signs, body weight and macroscopic observation at necropsy on Day 10. Rabbit specimens were fixed in 10% of neutral-buffered formalin and embedded in paraffin. Five μ m sections were then cut and mounted on glass slides, and histological evaluation of the tissues was performed by hematoxylin and eosin (H&E) staining. In addition, blood sampling for toxicokinetic evaluation was performed at the following time points: 0 (pre-dose) and 0.5 h, 1 h, 3 h, 6 h (Day 1), 24 h (Day 2), 48 h (Day 3), 120 h (Day 6) and 216 h (Day 10) after

dosing. The study was conducted by the Research Toxicology Centre (RTC, Pomezia, Italy). Procedures and facilities were compliant with the requirements of the Directive 2010/63/EU on the protection of animals used for scientific purposes. The national transposition of the Directive is defined in Decreto Legislativo 26/2014. RTC test facility is fully accredited by AAALAC. Aspects of the protocol concerning animal welfare have been approved by RTC animal-welfare body.

2.9. ELISA

Evaluation of the binding capacity of 1959, unconjugated 1959-sss and corresponding ADCs to Gal-3BP was performed by ELISA. Ninety-six well-plates NUNC were coated with human recombinant Gal-3BP (2 μ g/ml) overnight at 4 °C. After blocking with 1% BSA in PBS for 1 h, increasing concentrations of antibodies were added and incubated for 1 h at RT. After several washes with PBS-0.05% Tween-20, anti-human IgG-HRP (A0170, Sigma Aldrich) was added (1:5000) and incubated for 1 h at room temperature. After washes, stabilized chromogen was added for at least 10 min in the dark, before stopping the reaction with the addition of 1 N H₂SO₄. The resulting colour was read at 492 nm with an Elisa reader. K_d values were calculated using GraphPad Prism 5.0 software.

Circulating Gal-3BP in rabbit serum was measured by sandwich ELISA provided by DIESSE Diagnostica Senese Spa (Siena, Italy), following manufacturing instructions.

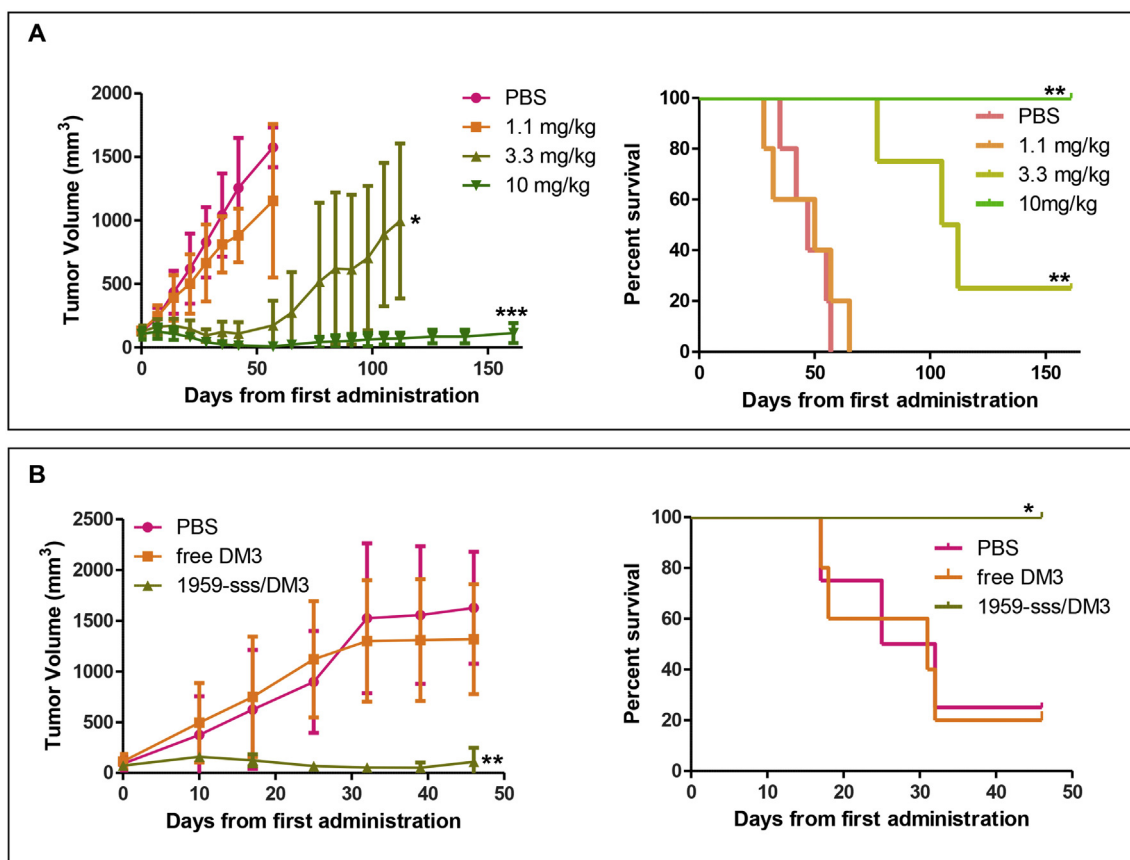


Fig. 3. 1959-sss/DM3 elicits dose-dependent antitumor activity. Tumor growth and Kaplan-Meier survival curves. (A) CD1 nude mice harboring melanoma A375m tumors were treated with increasing doses of 1959-sss/DM3 ADC (1.1, 3.3 and 10 mg/kg) for a total of five administrations twice weekly. $n = 5$ mice/group; $*p = .034$; $***p < .0001$. (B) Therapeutic activity of free DM3 (0.03 mg/kg), equivalent to the drug load on 1959-sss/DM3 at the dose of 3.3 mg/kg in A375m melanoma tumors. $n = 5$ mice/group; $*p = .022$; $**p = .033$. Control groups received PBS. Survival curves evaluated by Kaplan-Meier and analyzed by the log-rank test using Graphpad Prism 5 software.

2.10. Confocal imaging

Cells cultured under standard growth conditions were plated at 70% of confluence on glass coverslips and after 24 h were incubated with 10 $\mu\text{g}/\text{ml}$ of anti-Gal-3BP (1959) at 37 °C for 90 min in PBS and 3% of BSA. Afterwards the cells were washed in PBS, fixed in 4% paraformaldehyde, permeabilized and incubated with 1:200 AlexaFluor-488 conjugated anti-human IgG (A11013, Invitrogen, Life Technologies) and Hoechst 3342. Confocal images were acquired using a Zeiss LSM800 inverted confocal microscope system (Carl Zeiss, Gottingen, Germany). A single focal plane of the images was acquired under non-saturating conditions (pixel fluorescence below 255 arbitrary units) and using the same settings for all samples.

2.11. Immunohistochemistry

For the evaluation of Gal-3BP in human specimens, five-micrometer tissue sections of paraffin embedded blocks from eight invasive cancers (i.e. breast, colon, lung, stomach, urinary bladder, thyroid, prostate, and thymus; three cases examined for each tumor type), or corresponding adjacent non-tumorous, were stained for the Gal-3BP protein using the 1A4.22 monoclonal antibody [31]. Microwave pretreatment (10 min) in citrate buffer (pH 6.0) was performed for antigen retrieval. The Vectastain ABC peroxidase kit (Vector Laboratories, Burlingame CA) was used to detect the antigen. Endogenous biotin was saturated with a biotin blocking kit (Vector Laboratories). Negative controls were obtained using matched isotype control antibody.

2.12. Statistical analysis

For in vivo xenograft curves, P values were determined by Student's t -test and considered significant for $P < .05$. For Kaplan Meier survival analysis, a Log-rank (Mantel-Cox) test was used to compare each of the arms. Experimental sample numbers (n) are indicated in the Figure Legends. All statistical analysis was performed with GraphPad Prism 5.0 software.

3. Results

3.1. ADC generation and characterization

We aimed to develop linker-less non-internalizing ADCs targeting Gal-3BP. As first step, the murine anti-Gal-3BP antibody SP2 was humanized by CDR grafting as described previously [29] and in Materials and Methods. The resulting lead candidate, named 1959, was successively engineered into 1959-sss, where the three cysteines of the hinge region at 220, 226 and 229 are mutated into serine to allow site-specific disulfide linkages with thiol-maytansinoids at the C-terminal cysteine residue of each light chain (using a procedure published elsewhere) [6,30]. Binding to human recombinant Gal-3BP was similar for the three ADCs 1959-sss/DM1, 1959-sss/DM3, 1959-sss/DM4 and unconjugated 1959-sss. As determined by HIC, all ADC products displayed a DAR equal to 2. Their purity was judged optimal, as evaluated by SDS-PAGE, gel filtration, and mass spectrometric analysis (Fig. 1 and data not shown).

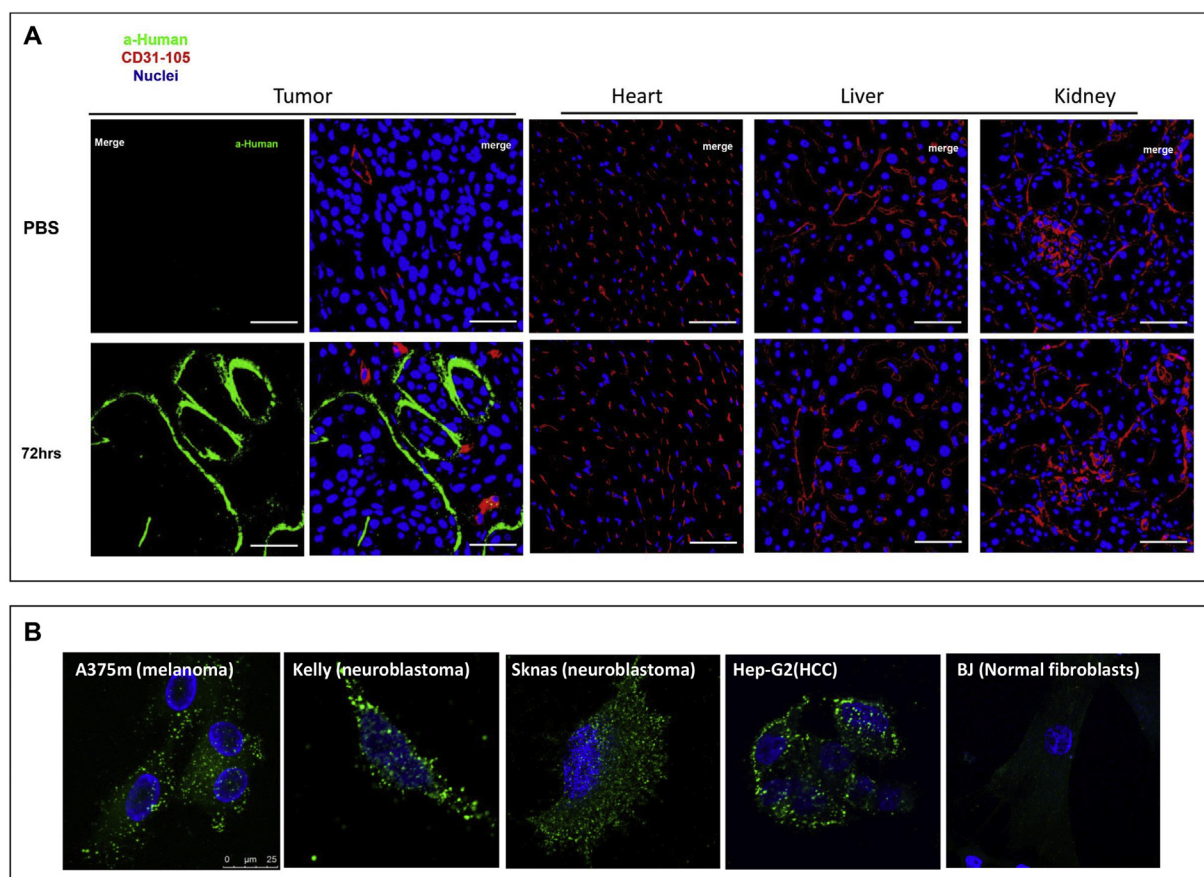


Fig. 4. 1959-sss/DM3 accumulates in tumor but not in normal tissues. (A) Representative images from tumor, heart, liver and kidney sections collected from mice treated with a single intravenous injection of 1959-sss/DM3 at the dose of 10 mg/kg or PBS (as control). After ADC was circulating for 72 h, mice tissues were excised and subjected to immunofluorescence staining. 1959-sss/DM3 was detected with anti-human IgG (green); blood vessels were stained using anti CD31/CD105 antibodies (red); cells nuclei were stained by DRAQ5 (blue). Scale bars: 50 μ m. (B) Staining of living tumor cells and BJ human fibroblasts with humanized 1959 anti-Gal-3BP antibody for 90 min at 37 °C followed by a fluorescent labelled secondary anti-human IgG antibody. (For interpretation of the references to colour in this figure legend, the reader is referred to the web version of this article.)

3.2. Therapeutic activity

The therapeutic activity of the ADC products was analyzed in mice harboring A375m human melanoma xenografts. In a first study, animals were treated daily for a total of 5 days at the dose of 10 mg/kg with either unconjugated 1959-sss, 1959-sss/DM1 or 1959-sss/DM3. Whilst negligible activity was observed for both unconjugated antibody and 1959-sss/DM1, a highly significant tumor growth inhibition associated with a prolonged survival was detected for 1959-sss/DM3 (Fig. 2A).

A second study was conducted in which different schedules of administration were evaluated. Mice harboring A375m human melanoma xenografts were treated with 10 mg/kg 1959-sss/DM3 daily or twice weekly for a total of 5 injections. A further experimental arm included animals receiving twice weekly injections of 10 mg/kg 1959-sss/DM4. As illustrated in Fig. 2B, a strong antitumor activity was confirmed in mice treated with daily injection of 1959-sss/DM3. However, a superior therapeutic activity, both in terms of tumor growth rate and survival was observed when this ADC was given twice weekly. Additionally, treatment twice weekly, but not daily was able to promote complete remission (CR), as measured 148 days from the start of ADCs administration. Overall, 1959-sss/DM3 resulted to be more efficient than 1959-sss/DM4 (CR 83% vs 50%, respectively). Based on these results, DM3-SH was chosen for further investigation.

We next evaluated the efficacy of 1959-sss/DM3 in a dose-response experiment in which animals were injected with 10 mg/kg, 3.3 mg/kg and 1.1 mg/kg of ADC twice weekly for a total of 5 injections. A quite

limited response was seen at the dose of 1.1 mg/kg, but a significant although not complete response was observed at the dose of 3.3 mg/kg. At the dose of 10 mg/kg, 100% of mice survival was observed at 160 days after start of treatment (Fig. 3A), confirming the high efficacy of this novel ADC. Importantly, 0.03 mg/kg of free DM3-SH, equivalent to the drug load of 3.3 mg/kg 1959-sss/DM3, had no effect on tumor growth (Fig. 3B).

3.3. ADC stability and safety

Mice tolerated well treatment with 1959-sss/DM3, as no significant body weight changes were observed in any of the above described experiments (Supplementary Fig. 2). Moreover, the ADC was found to be highly stable in vivo. MS analysis performed on serum of mice receiving 10 mg/kg of 1959-sss/DM3 or 0.1 mg/kg DM3-SH as control, revealed the presence of the free drug in the control animals (9–10 ng/ml) but not in those receiving the ADC (below the detection limit, data not shown).

As 1959 (and its engineered sss-variant) does not cross-react with murine Gal-3BP and to rule out the potential toxicity due to targeting the endogenous protein in healthy organs, we performed an exploratory toxicology study in rabbits, which is the only species, among the 15 different examined which displayed cross-reactivity with 1959/SP-2 antibody (our unpublished data). To this end, a single i.v. injection of 1959-sss/DM3 at the dose of 5 mg/kg was administrated in two rabbits, one male and one female. Endogenous level of circulating Gal-3BP was evaluated by ELISA and reported to be 350 \pm 17.4 ng/ml.

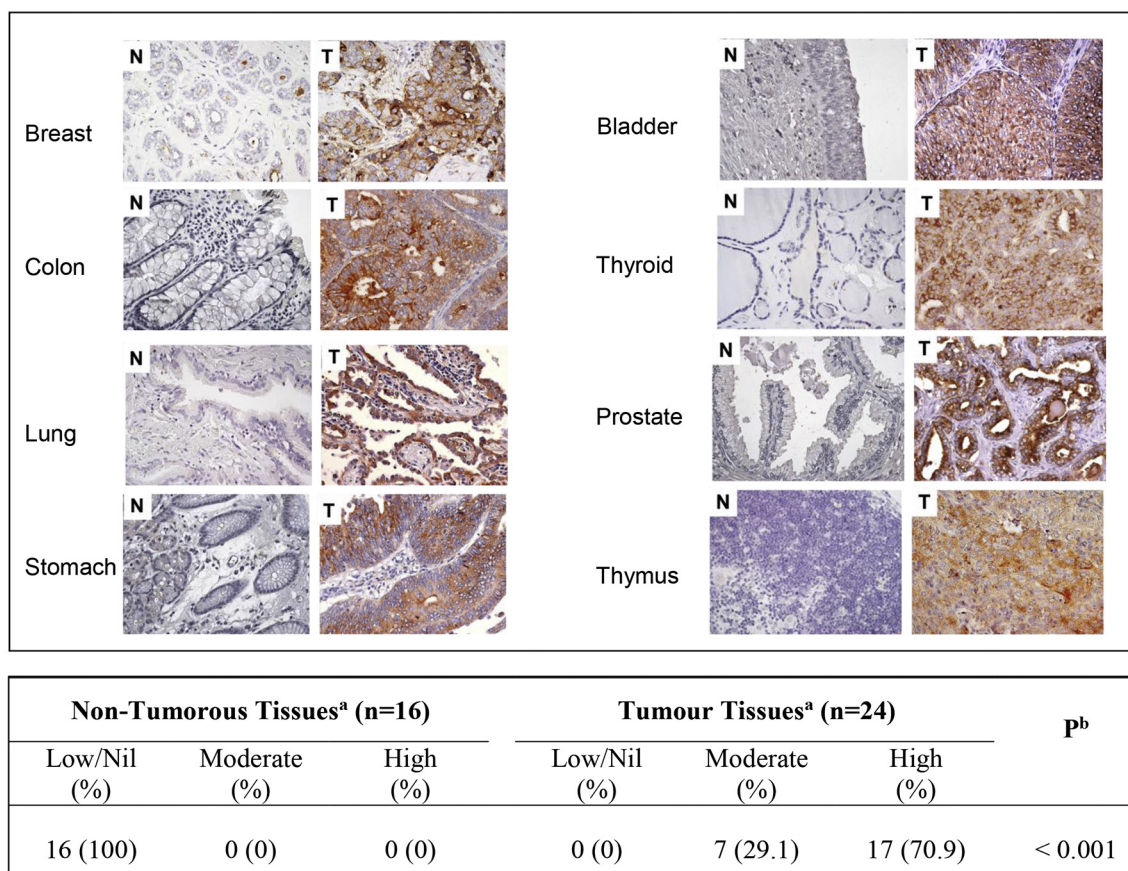


Fig. 5. Gal-3BP expression in human tumor tissues. A) Gal-3BP protein expression in a panel of human tumors (T) and non-tumorous tissues (N). Tissue sections were immunohistochemically stained with the anti-Gal-3BP 1A4.22 antibody. Original magnification 40 ×. B) Gal-3BP protein expression levels in tumors or corresponding non-neoplastic tissues^(a); Fisher's exact test analysis of non-tumorous versus tumor expression profile^(b). Two-tailed Fisher's exact tests was used to compare protein expression levels in non-tumorous versus tumor samples.

Importantly, no mortality or treatment-related toxicity signs were recorded during the study, and body weight resulted to be unaffected by the ADC administration (Supplementary Fig. 3).

3.4. Biodistribution and immunofluorescence analysis

We performed a biodistribution experiment in nude mice harboring xenografts of A375m using 1959-sss/DM3 at 10 mg/kg or PBS (as a control). Analysis of tissue staining 72 h after intravenous administration, revealed selective accumulation of the ADC at the tumor site, which was not observed for the control animals (Fig. 4A). Moreover, incubation of living tumor cells with the 1959 antibody (both wild type or in the -sss form) at 37 °C for 90 min followed by a fluorescent labelled secondary antibody revealed an intense pericellular staining, indicating translocation of the mature Gal-3BP protein across the membrane (Fig. 4B). Staining was not observed in normal human fibroblasts. These results indicated that the targeting of Gal-3BP by 1959-sss-ADCs occurred closely to tumor cells.

3.5. Gal-3BP expression in tumors

Next, we aimed at evaluating the expression of Gal-3BP in human tumors. To this end, an immunohistochemical analysis of Gal-3BP in human tumors (n = 24) versus non-tumorous tissues (n = 16) from individual patients was performed (Fig. 5A). Gal-3BP staining was cytoplasmic with diffuse and granular patterns (staining scale: Low/Nil = barely detectable intensity; Moderate = intermediate intensity; High = strong intensity). The Gal-3BP protein was upregulated in cancers (i.e. breast, colon, lung, stomach, urinary bladder, thyroid,

prostate, and thymus) versus their tissues of origin with high statistical significance (Fig. 5B). These data strengthen our previous findings where Gal-3BP expression resulted to be highly expressed in melanoma as compared with normal melanocytes [32]. This cancer-related expression included tissues of origin that were nil/low for Gal-3BP, which suggests selective pressure to increase Gal-3BP expression.

4. Discussion

ADC-based therapy is proving a huge success in the field of clinical oncology. Indeed, in addition to the four ADC already approved, there are many other compounds being tested in clinical trials [33].

Classically, ADCs have been developed using monoclonal antibodies with high internalizing capacity, in order to obtain an efficient delivery of the conjugated drug within the target cell. Recently, numerous studies have shown that this type of ADC can also function when the antibody does not internalize. The principle underlying this new approach is based on the fact that because of the reducing conditions, the payload can be released extracellularly, i.e. in the tumor microenvironment, where it diffuses inside the tumor cells provoking their death. Indeed, in the recent past several reports have documented that potent therapeutic activity can be obtained by targeting tumor or stroma cells components by non-internalizing ADC in different tumor models [5–8,32].

In the present paper, we confirm and extend these previous findings that cancer cures can be obtained without antibody internalization, by the targeted delivery of a suitable disulfide-linked ADC.

To the best of our knowledge, this is the first report of the induction of long-lasting complete remission in a xenograft model of cancer, using a non-internalizing ADC to a protein, such as Gal-3BP which is secreted

by cancer cells. Our ADC is based on an anti-Gal-3BP 1959 antibody engineered to contain one cysteine residue per light chain, which was coupled directly, without any linker to the thiol-containing drugs, DM1-SH, DM3-SH and DM4-SH. This procedure afforded product homogeneity with a defined DAR of 2. The conjugation strategy used in our study confirms previous works where linker-less ADC targeting alternatively spliced segments of the extracellular domain (EDA) of fibronectin displayed potent therapeutic activity in different tumor models [6,33].

Proteins such as Gal-3BP which are abundant and continuously secreted by tumor cells are easily accessible, which can significantly improve the accumulation and persistence of macromolecular ADC therapeutics at the site of disease. Following extravasation, ADCs which have bound to Gal-3BP at high concentration, closely to tumor cells, release the cytotoxic payloads which initiate tumor cell death. Released payloads may diffuse within the tumor mass, thus potentially reaching large numbers of cancer cells. The induction of tumor cell death may lead to a release of thiol substances, e.g. glutathione and cysteine which result in more drug release from the ADC, thus, triggering additional release of drug in a self-amplifying fashion.

The striking difference between the potent *in vivo* activity of ADCs containing DM3-SH or DM4-SH drugs and the low activity of the corresponding ADCs containing DM1 may be explained in terms of difference in the steric hindrance of the maytansinoid-based conjugates. According to literature data [34, 35], more hindered disulfide conjugates give higher potency and release maytansinoids at a slower rate, while are endowed with better stability. Also, antibody-maytansinoid conjugates with steric hindrance on the maytansinoid side of the disulfide bond, as in the case of 1959-sss/DM3 and 1959-sss/DM4 produces a higher bystander killing activity. It remains to be seen, however, to which extent preclinical findings observed in tumor-bearing mice may be predictive for the thiol-driven activation of ADCs in human malignancies, as concentration of the reducing substances could be different in the two species.

One aspect of relevance is the lack of cross reactivity of 1959 with the murine Gal-3BP, i.e. the target of the ADC. Therefore, one could speculate that serious toxicity issues may arise in the presence of the endogenous target in normal/healthy tissues of humans. However, our preliminary toxicity study in rabbits, a species cross reacting with 1959 antibody, seems to rule out such possibility, as no signs of toxicity were seen when 1959-sss/DM3 was administered at 5 mg/kg (corresponding to a dose even higher than the active dose used in therapy experiments).

Overall the findings of this study are innovative and of potential clinical relevance. They document that upon secretion, Gal-3BP localizes abundantly on cell surface, where it may become a suitable novel target of non-internalizing ADCs. The results of the immunohistochemical analysis (Fig. 5) and literature data revealed high expression of Gal-3BP in several malignancies, including non-small cell lung cancer [19], head and neck [36], breast cancer [37], prostate cancer [38], ovarian cancer [39] melanoma [40], lymphoma and neuroblastoma [41, 42], while being detectable at low level in most normal adult tissues. Therefore, conjugates between the 1959 antibody and the potent maytansinoid drugs, especially DM3-SH could be applicable to a wide range of tumor entities.

Supplementary data to this article can be found online at <https://doi.org/10.1016/j.jconrel.2018.12.018>.

Conflict of interests

Stefano Iacobelli is co-founder and shareholder of MediaPharma s.r.l.; Mauro Piantelli and Gianluca Sala are shareholders of MediaPharma s.r.l.; The other authors have no potential conflict of interest to disclose.

Funding

This project was funded in part by MediaPharma Srl; EC is recipient of an AIRC fellowship; GS is supported by AIRC (IG: 18467); VDL is supported by AIRC (IG: 20043).

Acknowledgments

We thank Cosmo Rossi for helping with animal studies, Annalisa Di Risio, Rossana La Sorda, Annalisa Nespole and Giulia Di Vittorio for technical assistance, Dr. Leonardo Sibilio for helpful discussion.

References

- [1] B.E. de Goeij, J.M. Lambert, New developments for antibody-drug conjugate-based therapeutic approaches, *Curr. Opin. Immunol.* 40 (2016) 14–23.
- [2] E.G. Kim, K.M. Kim, Strategies and advancement in antibody-drug conjugate optimization for targeted cancer therapeutics, *Biomol. Ther. (Seoul)* 23 (2015) 493–509.
- [3] K.R. Durbin, C. Phipps, X. Liao, Mechanistic modeling of antibody-drug conjugate internalization at the cellular level reveals inefficient processing steps, *Mol. Cancer Ther.* 17 (2018) 1341–1351.
- [4] E. Khera, C. Cilliers, S. Bhatnagar, G.M. Thurber, Computational transport analysis of antibody-drug conjugate bystander effects and payload tumoral distribution: implications for therapy, *Mol. Syst. Des. Eng.* 3 (2018) 73–88.
- [5] R. Gebleux, M. Stringhini, R. Casanova, A. Soltermann, D. Neri, Non-internalizing antibody-drug conjugates display potent anti-cancer activity upon proteolytic release of monomethyl auristatin E in the subendothelial extracellular matrix, *Int. J. Cancer* 140 (2017) 1670–1679.
- [6] E. Perrino, M. Steiner, N. Krall, G.J. Bernardes, F. Pretto, G. Casi, D. Neri, Curative properties of noninternalizing antibody-drug conjugates based on maytansinoids, *Cancer Res.* 74 (2014) 2569–2578.
- [7] S. Cazzamalli, B. Ziffels, F. Widmayer, P. Murer, G. Pellegrini, F. Pretto, S. Wulhfard, D. Neri, Enhanced therapeutic activity of non-internalizing small-molecule-drug conjugates targeting carbonic anhydrase ix in combination with targeted interleukin-2, *Clin. Cancer Res.* 24 (2018) 3656–3667.
- [8] A. Dal Corso, R. Gebleux, P. Murer, A. Soltermann, D. Neri, A non-internalizing antibody-drug conjugate based on an anthracycline payload displays potent therapeutic activity *in vivo*, *J. Control. Release* 264 (2017) 211–218.
- [9] G. Casi, D. Neri, Antibody-drug conjugates: basic concepts, examples and future perspectives, *J. Control. Release* 161 (2012) 422–428.
- [10] G.J. Bernardes, G. Casi, S. Trussel, I. Hartmann, K. Schwager, J. Scheuermann, D. Neri, A traceless vascular-targeting antibody-drug conjugate for cancer therapy, *Angew. Chem. Int. Ed. Engl.* 51 (2012) 941–944.
- [11] D. Neri, R. Bicknell, Tumor vascular targeting, *Nat. Rev. Cancer* 5 (2005) 436–446.
- [12] A. Ullrich, I. Sures, M. D'Egidio, B. Jallat, T.J. Powell, R. Herbst, A. Dreps, M. Azam, M. Rubinstein, C. Natoli, et al., The secreted tumor-associated antigen 90K is a potent immune stimulator, *J. Biol. Chem.* 269 (1994) 18401–18407.
- [13] G. Calabrese, I. Sures, F. Pompetti, G. Natoli, G. Palka, S. Iacobelli, The gene (LGALS3BP) encoding the serum protein 90K, associated with cancer and infection by the human immunodeficiency virus, maps at 17q25, *Cytogenet. Cell Genet.* 69 (1995) 223–225.
- [14] S. Iacobelli, I. Bucci, M. D'Egidio, C. Giuliani, C. Natoli, N. Tinari, M. Rubinstein, J. Schlessinger, Purification and characterization of a 90 kDa protein released from human tumors and tumor cell lines, *FEBS Lett.* 319 (1993) 59–65.
- [15] S. Iacobelli, E. Arno, A. D'Orazio, G. Coletti, Detection of antigens recognized by a novel monoclonal antibody in tissue and serum from patients with breast cancer, *Cancer Res.* 46 (1986) 3005–3010.
- [16] H. Inohara, A. Raz, Identification of human melanoma cellular and secreted ligands for galectin-3, *Biochem. Biophys. Res. Commun.* 201 (1994) 1366–1375.
- [17] I. Rosenber, B.J. Cherayil, K.J. Isselbacher, S. Pillai, Mac-2-binding glycoproteins. Putative ligands for a cytosolic beta-galactoside lectin, *J. Biol. Chem.* 266 (1991) 18731–18736.
- [18] F. Morandi, M.V. Corrias, I. Levreri, P. Scaruffi, L. Raffaghello, B. Carlini, P. Bocca, I. Prigione, S. Stigliani, L. Amoroso, S. Ferrone, V. Pistoia, Serum levels of cytoplasmic melanoma-associated antigen at diagnosis may predict clinical relapse in neuroblastoma patients, *Cancer Immunol. Immunother.* 60 (2011) 1485–1495.
- [19] A. Marchetti, N. Tinari, F. Buttitta, A. Chella, C.A. Angeletti, R. Sacco, F. Mucilli, A. Ullrich, S. Iacobelli, Expression of 90K (Mac-2 BP) correlates with distant metastasis and predicts survival in stage I non-small cell lung cancer patients, *Cancer Res.* 62 (2002) 2535–2539.
- [20] B.M. Kunzli, P.O. Berberat, Z.W. Zhu, M. Martignoni, J. Kleeff, A.A. Tempia-Caliera, M. Fukuda, A. Zimmermann, H. Friess, M.W. Buchler, Influences of the lysosomal associated membrane proteins (Lamp-1, Lamp-2) and Mac-2 binding protein (Mac-2-BP) on the prognosis of pancreatic carcinoma, *Cancer* 94 (2002) 228–239.
- [21] M. Correale, V. Giannuzzi, P.A. Iacovazzi, M.A. Valenza, S. Lanzillotta, I. Abbate, M. Quaranta, M.L. Caruso, S. Elba, O.G. Manghisi, Serum 90K/MAC-2BP glycoprotein levels in hepatocellular carcinoma and cirrhosis, *Anticancer Res.* 19 (1999) 3469–3472.
- [22] S. Iacobelli, P. Sismondi, M. Gai, M. D'Egidio, N. Tinari, C. Amatetti, P. Di Stefano, C. Natoli, Prognostic value of a novel circulating serum 90K antigen in breast

- cancer, *Br. J. Cancer* 69 (1994) 172–176.
- [23] S.Y. Park, S. Yoon, E.G. Sun, R. Zhou, J.A. Bae, Y.W. Seo, J.I. Chae, M.J. Paik, H.H. Ha, H. Kim, K.K. Kim, Glycoprotein 90K promotes e-cadherin degradation in a cell density-dependent manner via dissociation of e-cadherin-p120-catenin complex, *Int. J. Mol. Sci.* 18 (2017).
- [24] N. Tinari, I. Kuwabara, M.E. Huflejt, P.F. Shen, S. Iacobelli, F.T. Liu, Glycoprotein 90K/MAC-2BP interacts with galectin-1 and mediates galectin-1-induced cell aggregation, *Int. J. Cancer* 91 (2001) 167–172.
- [25] S. Traini, E. Piccolo, N. Tinari, C. Rossi, R. La Sorda, F. Spinella, A. Bagnato, R. Lattanzio, M. D'Egidio, A. Di Risio, F. Tomao, A. Grassadonia, M. Piantelli, C. Natoli, S. Iacobelli, Inhibition of tumor growth and angiogenesis by SP-2, an anti-lectin, galactoside-binding soluble 3 binding protein (LGALS3BP) antibody, *Mol. Cancer Ther.* 13 (2014) 916–925.
- [26] E. Piccolo, N. Tinari, D. Semeraro, S. Traini, I. Fichera, A. Cumashi, R. La Sorda, F. Spinella, A. Bagnato, R. Lattanzio, M. D'Egidio, A. Di Risio, P. Stampolidis, M. Piantelli, C. Natoli, A. Ullrich, S. Iacobelli, LGALS3BP, lectin galactoside-binding soluble 3 binding protein, induces vascular endothelial growth factor in human breast cancer cells and promotes angiogenesis, *J. Mol. Med. (Berl.)* 91 (2013) 83–94.
- [27] N. Tinari, M. D'Egidio, S. Iacobelli, M. Bowen, G. Starling, C. Seachord, R. Darveau, A. Aruffo, Identification of the tumor antigen 90K domains recognized by monoclonal antibodies SP2 and L3 and preparation and characterization of novel anti-90K monoclonal antibodies, *Biochem. Biophys. Res. Commun.* 232 (1997) 367–372.
- [28] E. Capone, E. Piccolo, I. Fichera, P. Ciufici, D. Barcaroli, A. Sala, V. De Laurenzi, V. Iacobelli, S. Iacobelli, G. Sala, Generation of a novel Antibody-Drug Conjugate targeting endosialin: potent and durable antitumor response in sarcoma, *Oncotarget* 8 (2017) 60368–60377.
- [29] G. Sala, I.G. Rapposelli, R. Ghasemi, E. Piccolo, S. Traini, E. Capone, C. Rossi, A. Pelliccia, A. Di Risio, M. D'Egidio, N. Tinari, R. Muraro, S. Iacobelli, C.I.N.p.I.B.-O. (CINBO), EV20, a novel anti-ErbB-3 humanized antibody, promotes ErbB-3 down-regulation and inhibits tumor growth in vivo, *Transl. Oncol.* 6 (2013) 676–684.
- [30] C.F. McDonagh, E. Turcott, L. Westendorf, J.B. Webster, S.C. Alley, K. Kim, J. Andreyka, I. Stone, K.J. Hamblett, J.A. Francisco, P. Carter, Engineered antibody-drug conjugates with defined sites and stoichiometries of drug attachment, *Protein Eng. Des. Sel.* 19 (2006) 299–307.
- [31] Y.S. Chang, E. di Tomaso, D.M. McDonald, R. Jones, R.K. Jain, L.L. Munn, Mosaic blood vessels in tumors: frequency of cancer cells in contact with flowing blood, *Proc. Natl. Acad. Sci. U. S. A.* 97 (2000) 14608–14613.
- [32] A.M. Cesinaro, C. Natoli, A. Grassadonia, N. Tinari, S. Iacobelli, G.P. Trentini, Expression of the 90K tumor-associated protein in benign and malignant melanocytic lesions, *J. Invest. Dermatol.* 119 (2002) 187–190.
- [33] C. Chalouni, S. Doll, Fate of antibody-drug conjugates in cancer cells, *J. Exp. Clin. Cancer Res.* 37 (2018) 20.
- [34] R. Gebleux, S. Wulhfard, G. Casi, D. Neri, Antibody Format and Drug Release Rate Determine the Therapeutic Activity of Noninternalizing Antibody-Drug Conjugates, *Mol. Cancer Ther.* 14 (2015) 2606–2612.
- [35] F. Dosio, P. Brusa, L. Cattel, Immunotoxins and anticancer drug conjugate assemblies: the role of the linkage between components, *Toxins (Basel)* 3 (2011) 848–883.
- [36] B.A. Kellogg, L. Garrett, Y. Kovtun, K.C. Lai, B. Leece, M. Miller, G. Payne, R. Steeves, K.R. Whiteman, W. Widdison, H. Xie, R. Singh, R.V.J. Chari, J.M. Lambert, R.J. Lutz, Disulfide-Linked Antibody–Maytansinoid Conjugates: Optimization of In Vivo Activity by Varying the Steric Hindrance at Carbon Atoms Adjacent to the Disulfide Linkage, *Bioconjugate Chemistry* 22 (2011) 717–727.
- [37] H. Endo, T. Muramatsu, M. Furuta, N. Uzawa, A. Pimkhaokham, T. Amagasa, J. Inazawa, K. Kozaki, Potential of tumor-suppressive miR-596 targeting LGALS3BP as a therapeutic agent in oral cancer, *Carcinogenesis* 34 (2013) 560–569.
- [38] N. Tinari, R. Lattanzio, P. Querzoli, C. Natoli, A. Grassadonia, S. Alberti, M. Hubalek, D. Reimer, I. Nenci, P. Bruzzi, M. Piantelli, S. Iacobelli, High expression of 90K (Mac-2 BP) is associated with poor survival in node-negative breast cancer patients not receiving adjuvant systemic therapies, *Int. J. Cancer* 124 (2009) 333–338.
- [39] E.L. Bair, R.B. Nagle, T.A. Ulmer, S. Laferte, G.T. Bowden, 90K/Mac-2 binding protein is expressed in prostate cancer and induces promatrilysin expression, *Prostate* 66 (2006) 283–293.
- [40] C. Escrevente, N. Grammel, S. Kandzia, J. Zeiser, E.M. Tranfield, H.S. Conrad, J. Costa, Sialoglycoproteins and N-glycans from secreted exosomes of ovarian carcinoma cells, *PLoS One* 8 (2013) e78631.
- [41] A.M. Silverman, R. Nakata, H. Shimada, R. Sposto, Y.A. DeClerck, A galectin-3-dependent pathway upregulates interleukin-6 in the microenvironment of human neuroblastoma, *Cancer Res* 72 (2012) 2228–2238.
- [42] S.J. Kim, S.J. Lee, H.J. Sung, I.K. Choi, C.W. Choi, B.S. Kim, J.S. Kim, W. Yu, H.S. Hwang, I.S. Kim, Increased serum 90K and Galectin-3 expression are associated with advanced stage and a worse prognosis in diffuse large B-cell lymphomas, *Acta Haematol* 120 (2008) 211–216.